Anal. Chem. **2003,** *75,* 1590−1598

Infrared Multiphoton Dissociation of Alkali Metal-Coordinated Oligosaccharides

Yongming Xie and Carlito B. Lebrilla*

Department of Chemistry, University of California, Davis, California 95616

Infrared multiphoton dissociation (IRMPD) of alkali metal-coordinated oligosaccharides was obtained in a Fourier transform mass spectrometer. Fragmentation of the oligosaccharides was observed for Li^+- and Na^+-coordinated species. For larger alkali metal ions (K^+, Rb^+, and Cs^+), the major products were the alkali metal ions. IRMPD experiments were performed on milk oligosaccharides, and the dissociation thresholds were determined. The threshold values were found to differ for the isomers. It is suggested that the threshold may be useful for differentiating isomeric compounds. Additionally, oligosaccharide alditols from biological samples were analyzed. Comparison of the collision-induced dissociation (CID) and IRMPD spectra of oligosaccharide alditols revealed that IRMPD could be used as a complementary method to obtain structural information.

Tandem mass spectrometry[1−4] is an essential technique for the structural elucidation of biopolymers. While the mass provides rudimentary information regarding composition, tandem MS or specifically collision-induced dissociation (CID) is invaluable for providing sequence information and connectivity.[5−10] In the analyses of oligosaccharides, CID provides not only connectivity but also linkage and, in some cases, stereochemical information.[11−16] Although CID is invaluable for structural analyses, it has inherent limitations. The total energy imparted on the ion is limited by instrumentation design. The conversion of translational energy to internal energy is not uniform and varies considerably with the size of the ion, which in turn leads to varying fragmentation efficiencies. Ion loss due to scattering decreases the sensitivity of the method.[17] Multiple MS events that are often necessary to provide extensive fragmentation are rendered ineffective by the extensive material losses during each CID event.

In Fourier transform ion cyclotron resonance mass spectrometry (FTICR-MS), CID further limits the accumulation time because each event adds an additional period to allow the removal of the collision gas. Infrared multiphoton dissociation (IRMPD) provides essentially the same fragment ions as CID,[18] but the technique has distinct advantages. IRMPD experiments have higher duty cycles than CID because the latter employs a collision gas that requires a pump-down period. Higher duty cycles allow more scans to be accumulated for a given duration.

IRMPD is well-suited for ion-storage mass analyzers. The IRMPD analyses of several small compounds have long ago been reported using FTICR-MS.[19−23] More recently, studies of IRMPD of proteins employing FTICR-MS have also been reported.[24−26] De novo sequencing of proteins, often with 100% sequence coverage, was demonstrated with IRMPD.[24] Similar capabilities with DNA and nucleotides were also demonstrated.[8,24,27,28] Nucleotides were also dissociated in an external ion reservoir of an FTICR mass spectrometer.[29] Phosphorylated peptides were similarly examined in the negative mode.[30] IRMPD has also been

* To whom correspondence should be addressed. E-mail: cblebrilla@ucdavis.edu.

(1) Cooks, R. G. *Collision Spectroscopy*; Plenum Press: New York, 1978.
(2) McLafferty, F. W. *Science* **1981**, *214*, 280−287.
(3) McLafferty, F. W. *Tandem Mass Spectrometry*; Wiley: New York, 1983.
(4) Busch, K. L.; Glish, G. L.; McLuckey, S. A. *Mass Spectrometry/Mass Spectrometry: Techniques and Applications of Tandem Mass Spectrometry*; VCH Publishers: New York, 1988.
(5) Guan, S. H.; Marshall, A. G.; Wahl, M. C. *Anal. Chem.* **1994**, *66*, 1363−1367.
(6) Hofstadler, S. A.; Wahl, J. H.; Bakhtiar, R.; Anderson, G. A.; Bruce, J. E.; Smith, R. D. *J. Am. Soc. Mass Spectrom.* **1994**, *5*, 894−899.
(7) Senko, M. W.; Speir, J. P.; McLafferty, F. W. *Anal. Chem.* **1994**, *66*, 2801−2808.
(8) Little, D. P.; Aaserud, D. J.; Valaskovic, G. A.; McLafferty, F. W. *J. Am. Chem. Soc.* **1996**, *118*, 9352−9359.
(9) Williams, E. R. *Anal. Chem.* **1998**, *70*, 179a−185a.
(10) Kelleher, N. L.; Lin, H. Y.; Valaskovic, G. A.; Aaserud, D. J.; Fridriksson, E. K.; McLafferty, F. W. *J. Am. Chem. Soc.* **1999**, *121*, 806−812.
(11) Domon, B.; Muller, D. R.; Richter, W. J. *Org. Mass Spectrom.* **1989**, *24*, 357−359.
(12) Orlando, R.; Bush, C. A.; Fenselau, C. *Biomed. Environ. Mass Spectrom.* **1990**, *19*, 747−754.
(13) Tseng, K.; Lindsay, L. L.; Penn, S.; Hedrick, J. L.; Lebrilla, C. B. *Anal. Biochem.* **1997**, *250*, 18−28.
(14) Weiskopf, A. S.; Vouros, P.; Harvey, D. J. *Rapid Commun. Mass Spectrom.* **1997**, *11*, 1493−1504.
(15) Konig, S.; Leary, J. A. *J. Am. Soc. Mass Spectrom.* **1998**, *9*, 1125−1134.
(16) Viseux, N.; de Hoffmann, E.; Domon, B. *Anal. Chem.* **1998**, *70*, 4951−4959.
(17) Williams, E. R.; Furlong, J. J. P.; Mclafferty, F. W. *J. Am. Soc. Mass Spectrom.* **1990**, *1*, 288−294.
(18) Gauthier, J. W.; Trautman, T. R.; Jacobson, D. B. *Anal. Chim. Acta* **1991**, *246*, 211−225.
(19) Morgenthaler, L. N.; Eyler, J. R. *J. Chem. Phys.* **1979**, *71*, 1486-1491.
(20) Burnier, R. C.; Cody, R. B.; Freiser, B. S. *J. Am. Chem. Soc.* **1982**, *104*, 7436−7441.
(21) Dunbar, R. C. *Gas-Phase Ion Chemistry*; **1984**, *3*, 130.
(22) Thorne, L. R.; Beauchamp, J. L. *Gas-Phase Ion Chemistry*, **1984**, *3*, 42.
(23) Bensimon, M.; Rapin, J.; Gaumann, T. *Int. J. Mass Spectrom. Ion Proc.* **1986**, *72*, 125−135.
(24) Little, D. P.; Speir, J. P.; Senko, M. W.; O'Connor, P. B.; McLafferty, F. W. *Anal. Chem.* **1994**, *66*, 2809−2815.
(25) Aaserud, D. J.; Little, D. P.; O'Connor, P. B.; McLafferty, F. W. *Rapid Commun. Mass Spectrom.* **1995**, *9*, 871−876.
(26) Dufresne, C. P.; Wood, T. D.; Hendrickson, C. L. *J. Am. Soc. Mass Spectrom.* **1998**, *9*, 1222−1225.
(27) Little, D. P.; McLafferty, F. W. *J. Am. Chem. Soc.* **1995**, *117*, 6783−6784.
(28) Little, D. P.; McLafferty, F. W. *J. Am. Soc. Mass Spectrom.* **1996**, *7*, 209−210.
(29) Hofstadler, S. A.; Sannes-Lowery, K. A.; Griffey, R. H. *Anal. Chem.* **1999**, *71*, 2067−2070.
(30) Flora, J. W.; Muddiman, D. C. *Anal. Chem.* **2001**, *73*, 3305−3311.

10.1021/ac026009w CCC: $25.00 © 2003 American Chemical Society
Published on Web 02/28/2003

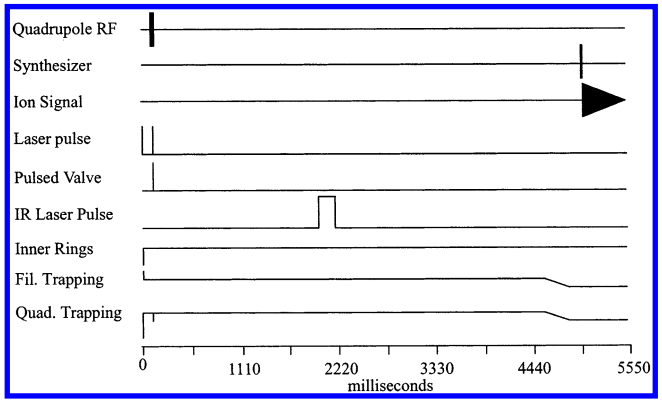

Figure 1. Pulse sequence employed for IRMPD experiment in FTICR mass spectrometer.

implemented on quadrupole ion trap (QIT) mass spectrometers.[31−35] However, because of the relatively higher pressure, it was necessary to heat the spectrometer so that collisions did not damp too significantly the internal energy of the IR-excited ions.[34] Alternatively, instead of continuous infusion, pulsed introduction of helium gas was used to lower the pressure in the ion trap and improve the efficiency of IRMPD.[32]

Recently, Costello and co-workers showed that IRMPD provides fragments of the glycan components of glycopeptides, leaving the peptide portion intact under certain conditions.[36] An earlier study used IRMPD to validate the structures of saccharomicins, which are heptadecaglycoside antibiotics.[37] These studies involved primarily protonated species of glycoconjugates. However, a great body of work is present on alkali metal coordinated species. Indeed, matrix-assisted laser desorption/ionization (MALDI)-produced ions are typically alkali metal-coordinated species.[13,38−41] The alkali metal ions also facilitate the determination of sequence, branching, and linkage.[13,38−41] An IRMPD-QIT-MS study of lithium-coordinated erythromycin analogues, which are small carbohydrate antibiotics with one or two monosaccharides attached,[35] has been published. However, there have been no systematic IRMPD studies involving larger oligosaccharides with various alkali metal ions.

In this report, we examined the general utility of IRMPD for the analyses of alkali metal-coordinated oligosaccharides. Although it has been reported that CID and IRMPD yield similar fragments,[18] there have been no studies that directly compare CID and IRMPD for alkali metal-coordinated oligosaccharide ions. One concern is the extent of fragmentation; IRMPD may provide more extensive fragmentation because the resulting fragment ions remain in the beam path, making further fragmentations likely.[37,42] There is also the issue of whether IRMPD will yield structurally relevant fragments or simply uninteresting small ions and the loss of alkali metal ions.

EXPERIMENTAL SECTION

Materials. Maltohexaose was obtained from Sigma Chemical Co. (St. Louis, MO). Permethylated maltohexaose was prepared using the procedure outlined in a previous study.[43] Milk oligosaccharides were obtained from Oxford Glycosystems (Oxford, U.K.). *O*-Linked oligosaccharide alditols were isolated from egg jelly glycoproteins of the South African toad, *Xenopus laevis*. The procedure was described in previous publications from this laboratory.[13,41,44,45] The matrix, 2,5-dihydroxybenzoic acid (DHB), was obtained from Aldrich Chemical Co. (Milwaukee, WI). All reagents were purchased in the highest purity and used without further purification.

For MALDI-FTMS experiments, all of the milk oligosaccharides were prepared as 0.1 mg/mL solutions in water. Other oligosaccharides were used as prepared in either water or water/acetonitrile solution. One microliter of sample solution was placed on the MALDI probe, and 1 μL of 0.01 M alkali metal salts was added to enrich the alkali metal ion concentration and produce primarily the corresponding alkali metal-coordinated species. One microliter of 0.4 M DHB in ethanol was added as matrix. Warm forced air was used to quickly evaporate the mixture on the probe.

MALDI-FTMS. MALDI-FTMS analyses were performed on an IonSpec (Irvine, CA) instrument equipped with a 4.7-T superconducting magnet. The details of the instrument are published elsewhere.[40,46] The instrument was also equipped with a nitrogen laser (337 nm) for desorption as standard equipment. The ions generated in the external source were transported through the quadrupole ion guide into the ICR cell and cooled by the argon gas introduced into the ICR cell by a pulse valve. CID and IRMPD experiments were performed on the ions trapped in the ICR cell.

All CID experiments were performed in the off-resonance mode. The desired ion was isolated in the ICR cell with the use of an arbitrary waveform generator and a frequency synthesizer. The ions were excited at 1000 Hz higher than their cyclotron frequency for 1000 ms at 2−7 V (base to peak), depending on the desired level of fragmentation and the size of the oligosaccharides. Two argon pulses were used during the CID event to maintain a pressure of 10^{-5} Torr.

To perform IRMPD experiments, modifications were carried out on the ICR cell by removing the trapping plate where the electron filament (for electron ionization) was mounted and replacing it with a copper plate containing a 13.3-mm hole in the center. Four pieces of copper wires (0.24 gauge) were fixed by screws onto the plate, two horizontally and two vertically over the hole and set 3.6 mm apart. The existing aluminum vacuum

(31) Colorado, A.; Shen, J. X.; Vartanian, V. H.; Brodbelt, J. *Anal. Chem.* **1996**, *68*, 4033−4043.
(32) Boue, S. M.; Stephenson, J. L., Jr.; Yost, R. A. *Rapid. Commun. Mass Spectrom.* **2000**, *14*, 1391−1397.
(33) Goolsby, B. J.; Brodbelt, J. S. *Anal. Chem.* **2001**, *73*, 1270−1276.
(34) Payne, A. H.; Glish, G. L. *Anal. Chem.* **2001**, *73*, 3542−3548.
(35) Crowe, M. C.; Brodbelt, J. S.; Goolsby, B. J.; Hergenrother, P. *J. Am. Soc. Mass Spectrom.* **2002**, *13*, 630−649.
(36) Hakansson, K.; Cooper, H. J.; Emmett, M. R.; Costello, C. E.; Marshall, A. G.; Nilsson, C. L. *Anal. Chem.* **2001**, *73*, 4530−4536.
(37) Shi, S. D. H.; Hendrickson, C. L.; Marshall, A. G.; Siegel, M. M.; Kong, F. M.; Carter, G. T. *J. Am. Soc. Mass Spectrom.* **1999**, *10*, 1285−1290.
(38) Cancilla, M. T.; Penn, S. G.; Carroll, J. A.; Lebrilla, C. B. *J. Am. Chem. Soc.* **1996**, *118*, 6736−6745.
(39) Harvey, D. J. *Mass Spectrom. Rev.* **1999**, *18*, 349−450.
(40) Cancilla, M. T.; Wang, A. W.; Voss, L. R.; Lebrilla, C. B. *Anal. Chem.* **1999**, *71*, 3206−3218.
(41) Tseng, K.; Hedrick, J. L.; Lebrilla, C. B. *Anal. Chem.* **1999**, *71*, 3747−3754.
(42) Jockusch, R. A.; Paech, K.; Williams, E. R. *J. Phys. Chem. A* **2000**, *104*, 3188−3196.
(43) Ahn, S.; Ramirez, J.; Grigorean, G.; Lebrilla, C. B. *J. Am. Soc. Mass Spectrom.* **2001**, *12*, 278−287.
(44) Tseng, K.; Xie, Y.; Seeley, J.; Hedrick, J. L.; Lebrilla, C. B. *Glycoconj. J.* **2001**, *18*, 309−320.
(45) Xie, Y. M.; Tseng, K.; Lebrilla, C. B.; Hedrick, J. L. *J. Am. Soc. Mass Spectrom.* **2001**, *12*, 877−884.
(46) Cancilla, M. T.; Penn, S. G.; Lebrilla, C. B. *Anal. Chem.* **1998**, *70*, 663−672.

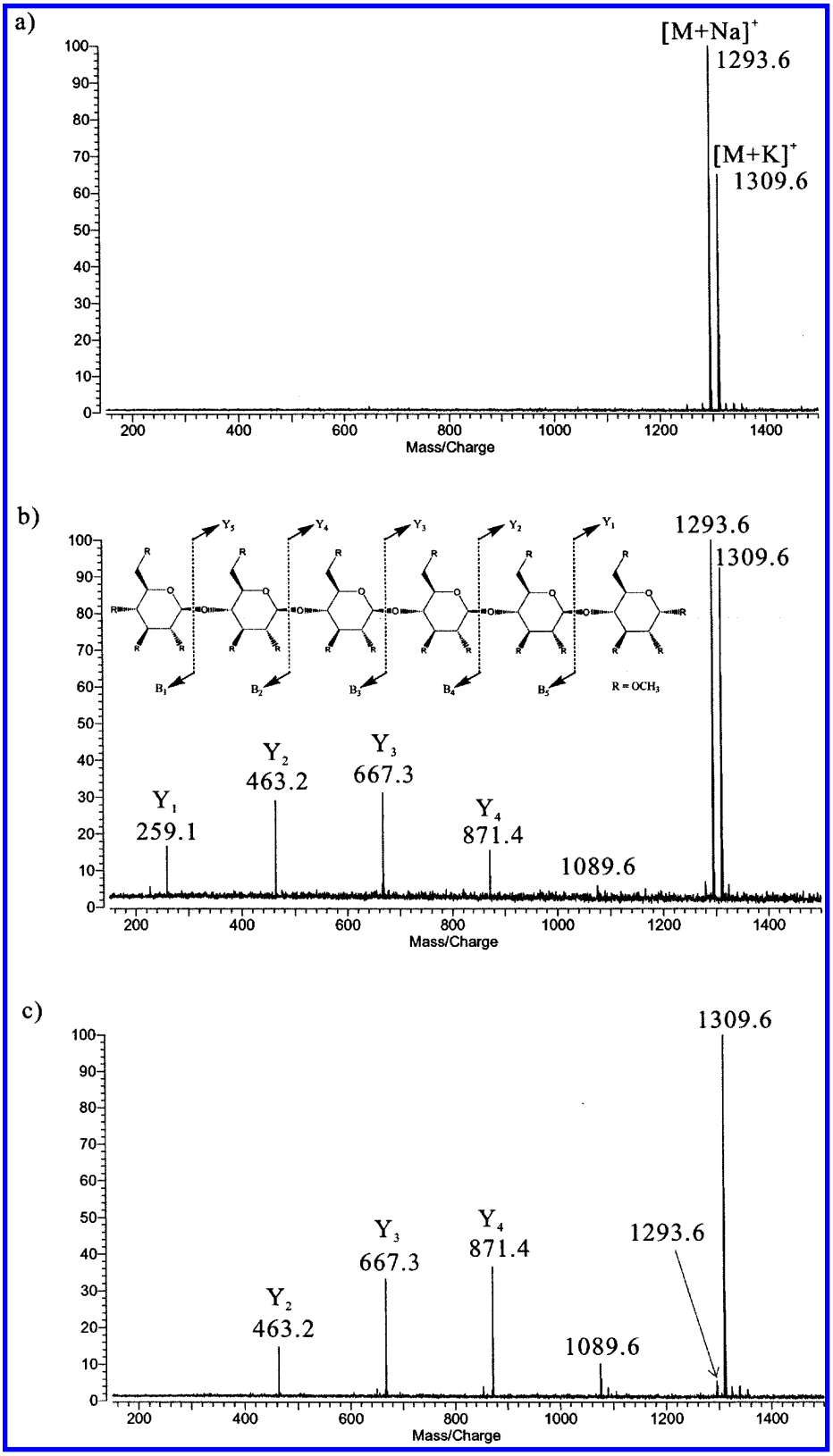

Figure 2. (a) MALDI-FTMS spectrum of permethylated maltohexaose with isolation of quasimolecular ions. Quasimolecular ions due to trace amounts of Na^+ and K^+ in the sample or the matrix used of Na^+ and K^+ are observed. (b) IRMPD mass spectrum of $[M + Na]^+$ and $[M + K]^+$ irradiated for 200 ms with 6 W. The fragments observed correspond primarily to Na^+-coordinated species. (c) Specific SORI-CID of $[M + Na]^+$ in the presence of $[M + K]^+$.

chamber was replaced with a smaller diameter (101.6 mm OD) tube containing a 70-mm BaF_2 window (Bicron Corp., Newbury, OH) at the end. A Parallax CO_2 laser (Waltham, MA) with 10.6-μm wavelength (0.1 eV per photon) and 20-W maximum power was mounted directly on the magnet and aimed toward the center of the analyzer cell.

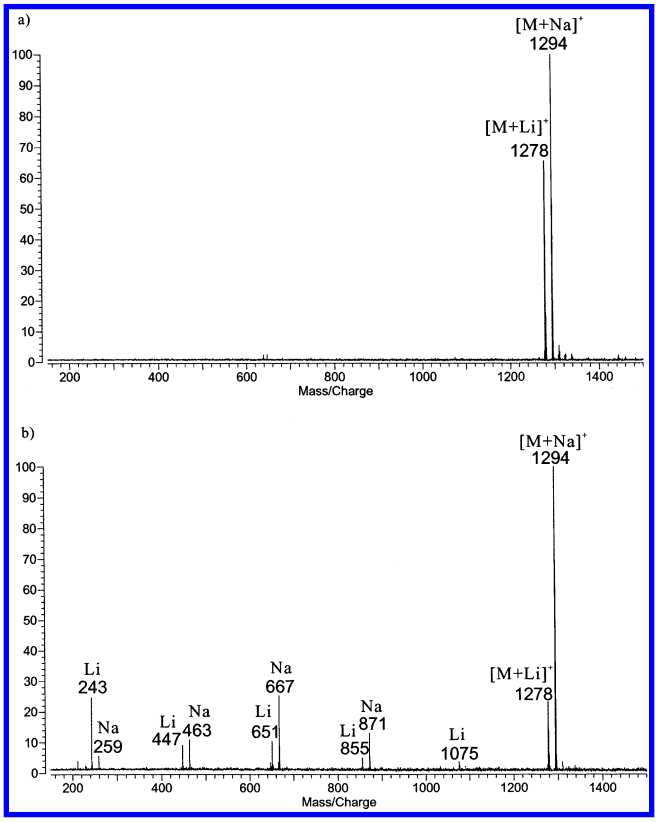

Figure 3. (a) MALDI-FTMS spectrum of permethylated maltohexaose doped with equal amounts of LiCl and NaCl. (b) IRMPD mass spectrum of isolated quasimolecular ions ($[M + Li]^+$ and $[M + Na]^+$). The fragments for Li^+- and Na^+-coordinated complexes are labeled as "Li" and "Na" separately.

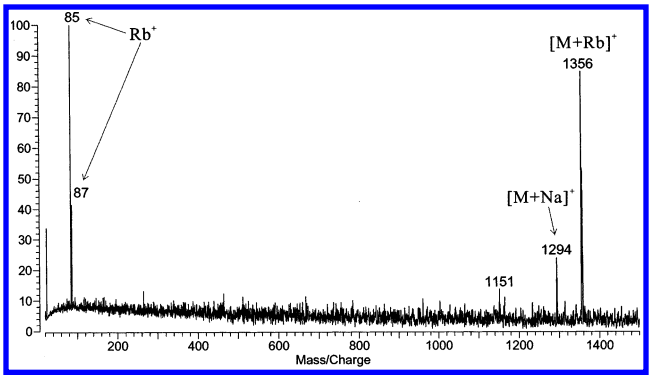

Figure 4. IRMPD mass spectrum of the RbCl-doped permethylated maltohexaose.

A typical pulse sequence for IRMPD is shown in Figure 1. The N_2 laser was fired twice at 0 and 100 ms as the quadrupole RF was turned on and the trapping plate closest to the quadrupole ion guide ("quad trapping", Figure 1) was timed to receive the ion. Two N_2 laser pulses were used for desorption. The first was used to activate the laser so that it could provide maximum power to the second pulse. By using two N_2 laser pulses, we found that the scan-to-scan reproducibility was greatly improved. The CO_2 laser was fired at 2000 ms with the trapping plates elevated to 20.0 V. The voltage was ramped down to 0.5 V at 4500 ms, and the ions were detected at 5000 ms. For the threshold time studies, the desired ions were isolated using a series of RF burst and sweep events between 1000 and 1500 ms.

RESULTS

It was found that the best IRMPD results were achieved with the laser beam positioned in the exact center of the cell. The beam had a manufacturer specification of 6 mm ($1/e^2$) diameter. This meant that the ion injection and trapping events, including the collisional cooling with Ar gas, kept the ions centered. Any event that would cause the ions to be removed from the center decreased the fragmentation efficiency. Similar phenomena were observed by Williams and co-workers.[42] Thus, ion isolation with either sweep events from a function generator or specific wave forms from an arbitrary waveform generator was carefully performed to maintain the desired ions relatively undisturbed in the center of the cell. For example, an isolation window of ±10 mass units produced only a small number of fragments, but increasing it to ±20 mass units produced abundant fragments. Employing the narrower mass window excited the desired ion to a larger orbit.

Space charge could also produce some scattering from the cell center.[42] We found that very intense signals did not produce IRMPD fragments readily. We surmised that ion repulsion due to space−charge interactions were sufficient to move the population of the ions off center, diminishing their interaction with the laser beam. A defocused laser beam may be useful in this situation by allowing a larger interaction volume.

IRMPD of Alkali Metal-Coordinated Maltohexaose. The MALDI-FTMS of permethylated maltohexaose yielded the spectrum shown in Figure 2a. For clarity, the region below m/z 1290 was swept out by a series of RF bursts and sweeps. Observed were the two quasimolecular ions corresponding to the Na^+- and the K^+-coordinated parent. The metal ions were obtained from trace amounts of Na^+ and K^+ in the sample or the matrix used because no NaCl was added during the sample preparation.

The IRMPD spectrum of the isolated Na^+- and the K^+-coordinated parent is shown in Figure 2b. To produce this spectrum, the laser was set to 6 W for a period of 200 ms. Setting the laser pulse longer than 1000 ms caused all signals to disappear. The fragment ion series, Y_n ($n = 1-4$), (according to the Domon and Costello nomenclature[47]) corresponded to only glycosidic bond cleavages of the Na^+-coordinated parent. The peak at m/z 1089.6 was believed to be a fragment due to the loss of one internal monosaccharide unit. Internal monosaccharide losses in both derivatized and underivatized oligosaccharides have been reported.[48−51]

Glycosidic bond cleavages in the K^+-coordinated species were not readily observed. The relative intensities of the Na^+- and the K^+-coordinated parents decreased upon irradiation, with the Na^+-coordinated parent decreasing more rapidly. It was determined that the dissociation products of the K^+-coordinated parents were mainly K^+ ions (see below). The CID of the sodiated parent (m/z 1293.6) from the mixture is shown for comparison (Figure 2c). Sustained off-resonance irradiation (SORI)-CID was used to selectively excite m/z 1293.6. The fragments in the two spectra (Figure 2b,c) are identical with the CID favoring the larger fragments and IRMPD favoring the smaller ones. The monosac-

(47) Domon, B.; Costello, C. E. *Glycoconj. J.* **1988**, *5*, 397−409.
(48) McNeil, M. *Carbohydr. Res.* **1983**, *123*, 31−40.
(49) Kovacik, V.; Hirsch, J.; Kovac, P.; Heerma, W.; Thomas-Oates, J.; Haverkamp, J. *J. Mass Spectrom.* **1995**, *30*, 949−958.
(50) Brull, L. P.; Heerma, W.; Thomas-Oates, J.; Haverkamp, J.; Kovacik, V.; Kovac, P. *J. Am. Soc. Mass Spectrom.* **1997**, *8*, 43−49.
(51) Franz, A. H.; Lebrilla, C. B. *J. Am. Soc. Mass Spectrom.* **2002**, *13*, 325−337.

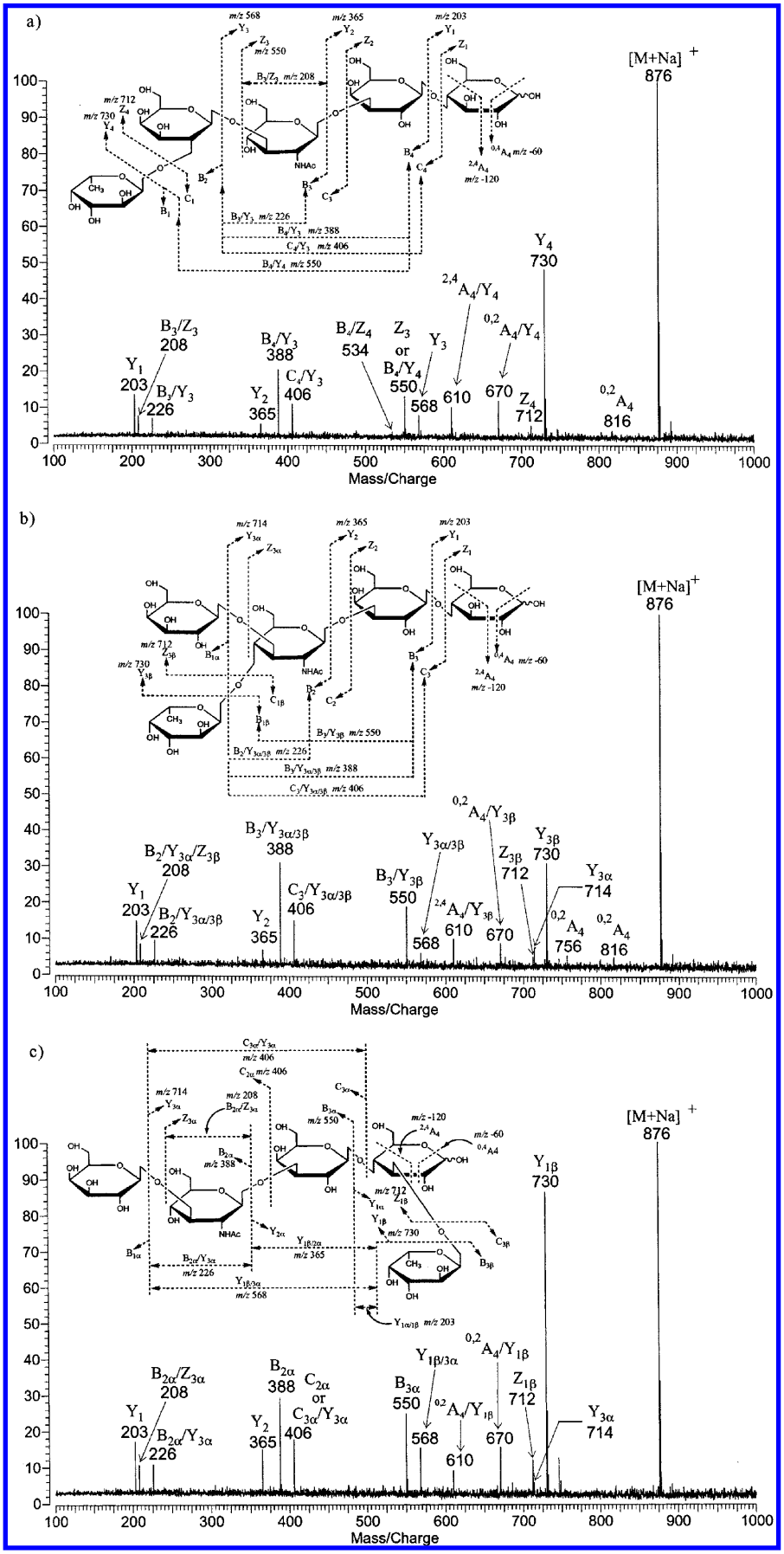

Figure 5. IRMPD mass spectra of (a) LNFP-I, (b) LNFP-II, and (c) LNFP-V. The samples were doped with NaCl. The structures are inserted with the fragmentation annotated.

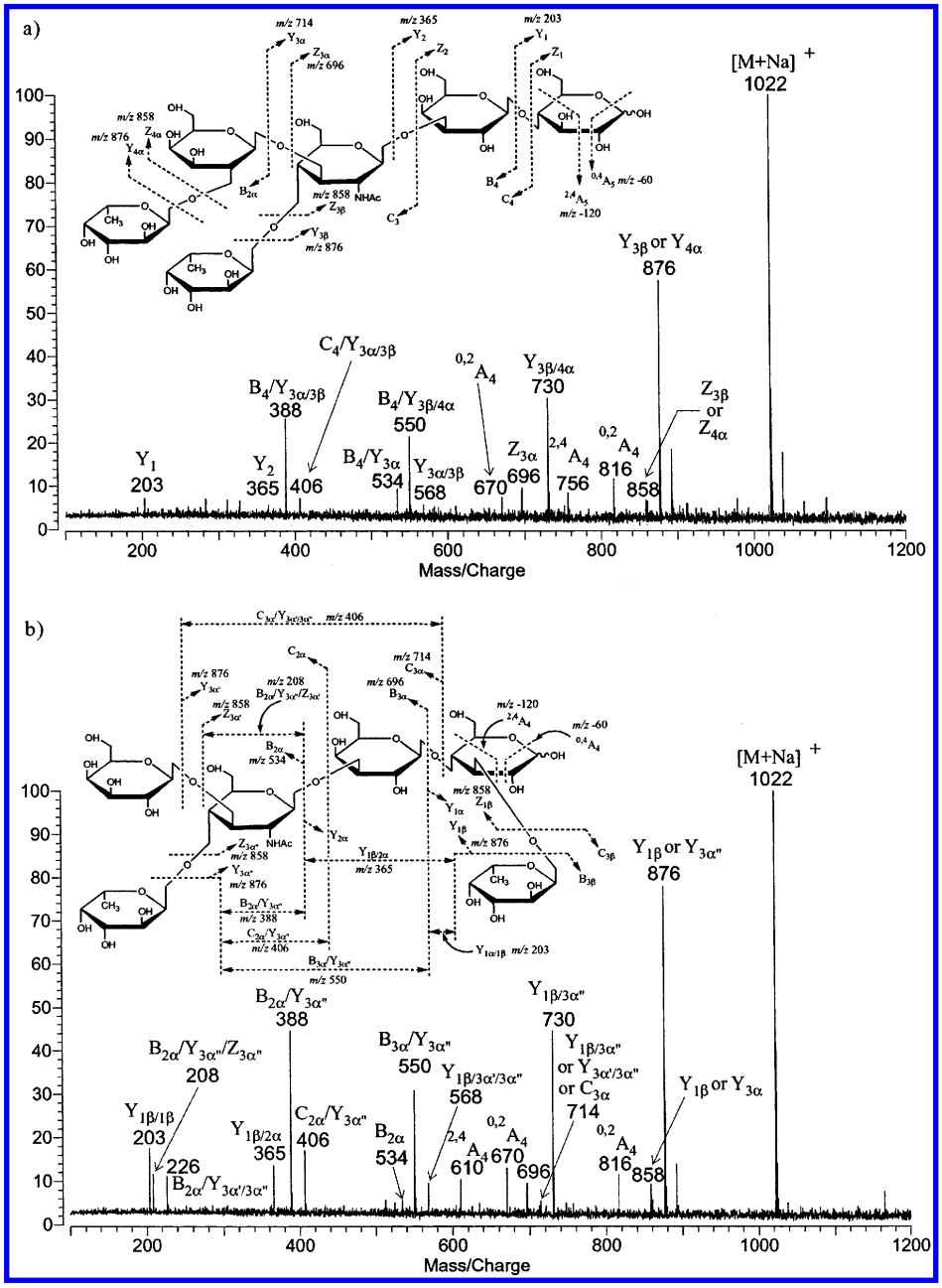

Figure 6. IRMPD mass spectra of (a) LNDFH-I and (b) LNDFH-II. The structures are inserted with the fragmentation annotated.

charide residue (m/z 259.1) is absent in the CID spectrum. More energetic conditions, such as higher RF amplitude or longer excitation time, produced the monosaccharide residue at the expense of the higher mass fragments and overall signal intensity in the CID spectra. The CID of the K^+-coordinated species also produced the corresponding fragments (spectrum not shown).

The lack of fragment ions with K^+-coordinated oligosaccharides encouraged us to examine other alkali metal ions. Experiments were performed with permethylated maltohexaose doped with equal amounts of LiCl and NaCl. The resulting MALDI-FTMS spectrum yielded quasimolecular ions with the Li^+-coordinated species being 65% as abundant as the Na^+-coordinated species (Figure 3a). IRMPD of the isolated quasimolecular ions yielded the spectrum shown in Figure 3b, in which both ionic series were observed. IRMPD conditions were the same as the previous experiments with the Na^+- and K^+-coordinated parent ions. The decreased amplitude of the Li^+-coordinated parent indicated they underwent much more extensive fragmentation than the Na^+-coordinated parent. This resulted in two different fragmentation profiles. The Li^+-coordinated fragments (m/z 243.1, 447.2, 651.3, and 855.4) and the Na^+-coordinated fragments (m/z 259.1, 463.2, 667.3, and 871.4) were observed. The distribution profile of the Li^+-coordinated fragments centered more toward the lower masses, with the single residue fragment being the most abundant. The Na^+-coordinated species centered on the trisaccharide fragment (m/z 667.3). IRMPD of the isolated Na^+- and Li^+-coordinated parents yielded similar results, that is, the Li^+-coordinated parent fragmented more extensively than the Na^+-species. Similar behavior was also observed in the CID experiments of Li^+- and Na^+-coordinated oligosaccharides.[40]

A systematic study was performed to determine whether the lack of fragment ions correlated with the sizes of alkali metal ions.

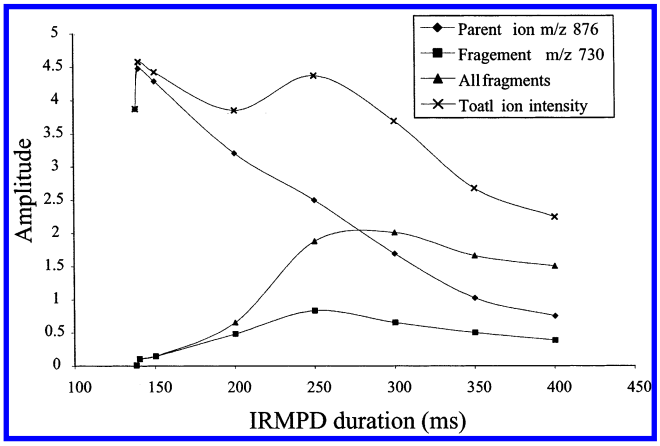

Figure 7. Plot of the sum of the ion intensities (not normalized) and the relative intensities of the quasimolecular ion $[M + Na]^+$, the fragment due to the loss of the fucose residue $[M + Na - Fuc]^+$, and the sum of all fragments as a function of the irradiation period for LNFP-I.

Table 1. Irradiation Thresholds for the Loss of Fucose Residues from the Quasimolecular Ion $[M + Na]^+$

compd	− 1 fucose (ms)	−2 fucose (ms)
LNFP-I	138 ± 3	
LNFP-II	133 ± 3	
LNFP-V	118 ± 3	
LNDFH-I	125 ± 3	190 ± 4
LNDFH-II	102 ± 3	135 ± 3

Maltohexaose samples were doped with specific alkali metal salts to produce the corresponding quasimolecular ions that were then examined by IRMPD. With Li^+ and Na^+, fragments were obtained in both IRMPD and CID spectra similar to those obtained in Figures 2 and 3. However, with K^+, Rb^+, and Cs^+, alkali metal-coordinated fragments were not readily observed. This behavior is illustrated with Rb^+. In Figure 4, the IRMPD spectrum of the RbCl doped sample is shown. The major product observed was Rb^+ (m/z 84.9 and 86.9), which was consistent with metal ion loss as the main channel for fragmentation. The peak at m/z 1293.6 corresponded to the sodiated parent. A weak signal at m/z 1151.4 corresponded to the loss of one monosaccharide unit from the Rb^+-coordinated parent. These two ions were present in the spectrum because of insufficient ion ejection. It was previously shown with CID that the relative proportion of the metal ion loss increased with the larger metals so that K^+ produced primarily fragmentation of the oligosaccharide, whereas Rb^+ and Cs^+ produced primarily metal ion dissociation.[40] It may be concluded that Li^+ and Na^+-coordinated species yielded primarily oligosaccharide fragments with IRMPD, but K^+, Rb^+, and Cs^+-coordinated species yielded only metal ions.

IRMPD of Oligosaccharides from Human Milk. Examination of more complicated oligosaccharide structures illustrated the general utility of IRMPD. Two sets of isomeric oligosaccharides were examined, including three pentasaccharides and two hexasaccharides. The pentasaccharides contained a common tetrasaccharide core composed of a glucose residue at the reducing end and a galactose residue at the nonreducing end. The linkage of the fucose varied slightly, being (α1-2)-linked to the nonreducing end for LNFP-I, (α1-4)-linked to the adjacent *N*-acetylglucosamine (LNFP-II), and (α1-3)-linked to the reducing end glucose (LNFP-V). The hexasaccharides contained the same pentasaccharide core with the second fucose on the nonreducing end galactose (α1-2)-linked for LNDFH-I and (α1-3)-linked to the reducing end glucose for LNDFH-II.

The IRMPD spectra of LNFP-I, LNFP-II, and LNFP-V were obtained for the sample doped with NaCl (Figure 5a,b,c). The major product ions were due to losses of fucose (m/z 730; for simplicity, only nominal masses will henceforth be provided). Fragments corresponding to both ion series y_n (b_n) and z_n (c_n) were observed. Fragments due to combinations of cleavages at both reducing and nonreducing ends were also observed. For example, b_m/z_n, and c_m/y_n combinations were present in the spectra. Additionally, cross-ring cleavages were also observed primarily at the reducing end glucose ($^{2,4}a_4$ and $^{0,2}a_4$). Cross-ring cleavages are desirable because they provide information regarding the linkages between the monosaccharide units.

It was difficult to distinguish the three LNFP isomers because the pentasaccharide isomers yielded very similar IRMPD spectra. There were, however, minor variations between these spectra. The major differences in the spectra occurred in the region between m/z 730 and 876, where products due to cross-ring cleavages of the reducing end were found. Cross-ring cleavage products were also found at lower masses as a result of multiple fragmentation events. For LNFP-I, a single product was observed corresponding to $^{0,2}a_4$ (m/z 816, Figure 5a). For LNFP-II, two product ions were observed corresponding to $^{2,4}a_4$ and $^{0,2}a_4$ (m/z 816 and 756, respectively, Figure 5b). For LNFP-V (Figure 5c), no product ions were observed in this mass range. Apparently, the fucose residue on the reducing end glucose inhibited cross-ring cleavages on the glucose. Note that once the fucose residue was lost, cross-ring cleavages were observed (m/z 610, and 670, Figure 5c).

An additionally informative peak was the loss of the galactose residue at the nonreducing end (m/z 714). This fragment was found with LNFP-II (Figure 5b) and LNFP-V (Figure 5c), but not with LNFP-I because of the fucose attached directly to the residue in the latter.

There were similarly small variations in the IRMPD spectra of the hexasaccharides LNDFH-I and LNDFH-II (Figure 6a,b). There were a number of peaks of weak intensities present in one spectrum but not the other. For example, under identical conditions, the ion m/z 756 was observed only in LNDFH-I, whereas m/z 226 and 208 where present only in LNDFH-II.

Dissociation Threshold of Oligosaccharide. The lack of more definite distinguishing features in the tandem MS spectra with both CID and IRMPD made the differentiation of individual isomers difficult. However, the variations in the linkage could potentially affect the energetics of the fragmentation reactions. To examine the energetics of fragmentation, the irradiation period was varied for each isomer to determine the dissociation threshold. The milk oligosaccharides were ideal compounds for this study because they vary only in the position and the linkage of the fucose. The fucose residue was the most labile under both CID and IRMPD; its loss was readily monitored.

Figure 7 shows the total sum of the ion intensities (not normalized) and the relative intensities of the quasimolecular ion $[M + Na]^+$, the fragment due to the loss of the fucose residue $[M + Na - Fuc]^+$, and the sum of all fragments as a function of the irradiation period for LNFP-I. There are two interesting features of the plots. First, the fragments were observed only after an irradiation period of ~140 ms. Second, a decrease in the total

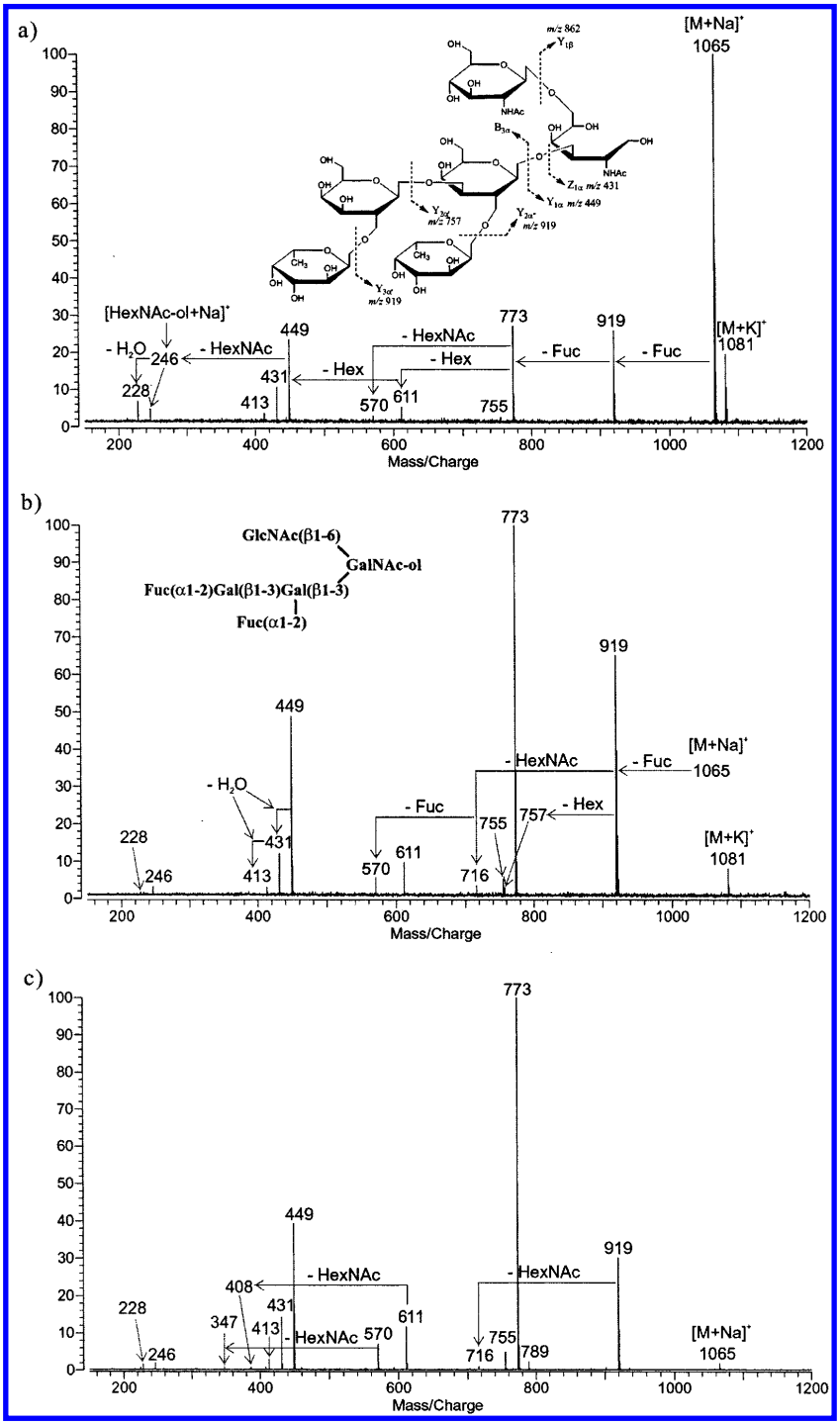

Figure 8. (a) IRMPD, (b) CID, and (c) in-source dissociation spectra of an *O*-linked oligosaccharide alditol (*m*/*z* 1065.4) isolated from egg jelly glycoproteins.

ion amplitude was observed at prolonged IR exposure, which indicated ion loss. Ions were "lost" when they fragmented to smaller species that were outside the mass range being monitored. The decrease of the total ion abundance was highly reproducible and observed even when the MALDI laser spot was varied along the probe surface.

Determining the fragmentation threshold is generally difficult. All experimental parameters were rigorously maintained from one determination to the next. We found that two major parameters varied the threshold, namely, the laser power and the alignment of the beam. We did not vary the matrix or the preparation conditions. For these determinations, we chose a simple criterion for threshold; it was defined by the S/N > 2. Although there are more rigorous methods for this determination,[42] they cannot be performed with the current experimental setup. The goal here was to examine primarily the variations in irradiation period as a function of structure.

The dissociation threshold varied with the position and the linkage of the fucose (Table 1). For each value in Table 1, three experiments were performed. For LNFP-I, with the fucose (α1-2)-linked to the galactose, the loss of the fucose appeared with a minimum irradiation period of 138 ms. For LNFP-II, with the

fucose (α1-4)-linked to the adjacent *N*-acetylglucosamine, the minimum irradiation period was 133 ms. For LNFP-V, with the fucose (α1-3)-linked to the reducing end glucose, the minimum irradiation period was 118 ms.

The differences in the irradiation thresholds between LNDFH-I and LNDFH-II were more pronounced. The loss of the first fucose required 125 ms for LNDFH-I and 102 ms for LNDFH-II. As expected, the loss of the second fucose would require greater irradiation periods. For LNDFH-I, 190 ms was required, whereas 135 ms was required for LNDFH-II.

The dissociation thresholds were reproducible from day to day if the beam alignment and the laser power were fixed. Varying the laser power varied the threshold but the relative order of the dissociation thresholds was maintained.

IRMPD of Oligosaccharide Alditols. The IRMPD of model compounds, those commercially available in pure forms (see above), do not necessarily illustrate the potential utility and possible pitfalls of the method. We therefore examined compounds that were isolated from biological sources, that is, mucin-type oligosaccharides from extracelluar matrix, for this report.[13,41,44,45] These *O*-linked glycans are most conveniently released as alditols, making the reducing end residue unique. Alditols often fragment from the nonreducing end first, leaving the alditol residue as the smallest observable fragment.[13,41] This allows the determination of the reducing end as being either a hexaose or a *N*-acetylhexaosamine. We have posited that the open alditol residue coordinates the alkali metal more strongly than the pyranose residues. The CID of the oligosaccharide alditols also tends to yield more distinguishing fragments than the corresponding aldehydes.[13,41] The CID spectra are very specific and can be used to identify the compound.[13,41]

The IRMPD spectrum of an *O*-linked oligosaccharide alditol (m/z 1065.4) isolated from the egg jelly glycoproteins of the South African toad, *Xenopus laevis*, is shown in Figure 8a. This spectrum contains nearly all of the same ions as the CID spectrum (Figure 8b). For comparison, the fragment ion spectra produced from elevated MALDI laser fluence, a type of "in-source dissociation" (ISD), is shown in Figure 8c. Note the absence of cross-ring cleavages in all of the spectra; they are typically not observed with reduced oligosaccharides. Generally, we find ISD to provide the most structurally useful fragment ions. For example, fragments $y_{1\beta}/y_{2\alpha'}/y_{2\alpha''}$ (m/z 408.2) and $b_{3\alpha}/y_{2\alpha''}/y_{3\alpha'}$ (m/z 347.1), which are two key fragments for determination of the structure, were missing in both IRMPD and CID spectra (Figure 8a and 8b). A major limitation of the ISD spectra is that structural elucidation is possible only with pure compounds.

A weakly abundant $y_{2\alpha'}$ (m/z 757.2) fragment, diagnostic of the Gal(β1-3)Gal linkage,[41] was not observed in the IRMPD but was observed as a weak signal in the CID spectrum. However, small fragments, like alditol residue ions (m/z 228.1 and 246.1) were clearly and consistently observed in the IRMPD spectra but were often absent in the CID spectra. In our experience, we found that compounds with molecular weight >1300 Da generally required more than two MS stages of CID to yield small fragments that correspond to the alditol residue. However, the IRMPD readily yielded the monosaccharide alditol residue in a single MS/MS event.

DISCUSSION

The two major reaction pathways under IRMPD are the loss of the metal (dissociation) and the fragmentation of the oligosaccharides. For the small alkali metals (Li^+ and Na^+), the major reaction products were due to fragmentation. For the large alkali metal ions, K^+, Rb^+, and Cs^+, the prominent reaction products observed were the alkali metal ions, corresponding primarily to dissociation. Similar behavior was observed in an extensive CID investigation reported earlier.[40] However, the differentiation between the two reaction channels was not as distinct in CID. Fragmentation reactions were observed prominently in CID even with K^+, Rb^+, and Cs^+, albeit the relative abundance of the bare metal ion increased with the size of the alkali metal.

The binding energy of the alkali metal to oligosaccharides decreases in the order $Li^+ > Na^+ > K^+ > Rb^+ > Cs^+$.[40] For this reason, alkali metal ion loss is greater for Cs^+ and less for Li^+. This order is also the same for the ability of the metal to catalyze charge-site fragmentation.[40] Li^+ and Na^+ produce more fragments than the larger alkali metal ions. It is conceivable that the reaction threshold is higher for metal ion loss than for fragmentation for Li^+ and Na^+. For the larger alkali metal ions, K^+, Rb^+, and Cs^+, the reverse is true. The metal ion dissociation has a lower threshold than fragmentation.

CONCLUSION

There are minor but critical differences between the (off-resonance) CID and IRMPD methods. For CID, the larger variations in energy transferred during collisions provide dissociation pathways that are not accessible to IRMPD. For this reason, CID yields both fragmentation and metal ion dissociation when the oligosaccharides are coordinated to larger alkali metal ions, such as K^+, Rb^+, and Cs^+. For these metals, IRMPD yields only dissociation. However, for smaller metals, such as Li^+ and Na^+, we found very little variations in the ions produced by the two methods. CID can potentially yield more characteristic ions that provide additional information. On the other hand, IRMPD provides energy not only to the isolated ions but also to the fragment ions to produce a cascade of fragments down to the last residue. For the oligosaccharide alditols, it allows the rapid determination of the reducing end. This information is accessible by CID, but usually only through multiple tandem MS events. In this regard, IRMPD and CID offer complementary information.

The fragmentation behavior of isomers has distinct energetics that may be differentiated by their dissociation thresholds. In situations in which CID and IRMPD spectra do not yield definitive peaks for structural differentiation, an IRMPD threshold may be valuable. IRMPD therefore provides another method in the toolbox needed for oligosaccharide analyses.

ACKNOWLEDGMENT

Funding provided by the National Science Foundation and the National Institutes of Health is gratefully acknowledged. The authors thank Michael Sisto, Jinghua Zhang, Scott Russell, and Kate Schubothe for their help with instrumental modification.

Received for review July 30, 2002. Accepted December 12, 2002.

AC026009W